Performance of Single-Carrier Frequency-Domain Adaptive Antenna Array

Byeong-woo Kang[1], Kazuaki Takeda[1], and Fumiyuki Adachi[2]
Dept. of Electrical and Communication Engineering, School of Engineering, Tohoku University, JAPAN
6-6-05 Aza-Aoba, Aramaki, Aoba-ku, Sendai, 980-8579 JAPAN
Email: [1]{kang, takeda}@mobile.ecei.tohoku.ac.jp [2] adachi@ecei.tohoku.ac.jp

***Abstract*— The bit error rate (BER) performance of single-carrier (SC) transmission in a frequency-selective fading channel can be significantly improved by using frequency-domain equalization (FDE). In a cellular network, however, the same frequency is reused in different cells to efficiently utilize the limited bandwidth and therefore, the BER performance degrades due to co-channel interference (CCI). Adaptive antenna array (AAA) is one of the well-known techniques to suppress the CCI. In this paper, we consider a frequency-domain AAA, based on the average CCI power minimization criterion, jointly used with FDE and theoretically derive the optimum array weight using Lagrange multiplier method. We evaluate, by the computer simulation, the outage probability of the BER in a frequency-selective CCI environment.**

***Index Terms*—** *Adaptive antenna array, frequency-domain equalization, outage probability, co-channel interference*

I. INTRODUCTION

In the next generation mobile communication systems, very high speed data services of 100 Mbps ~ 1 Gbps are demanded. For such a high speed data transmission, the channel becomes severely frequency-selective and produce severe inter-symbol interference (ISI), thereby significantly degrading the single-carrier (SC) transmission performance [1]. Recently, multi-carrier (MC) transmission [2] has been attracting much attention. However, the MC transmission has a problem of large peak-to-average power ratio (PAPR) and requires expensive linear transmit power amplifiers at mobile terminals. SC transmission has been considered again, but with the application of frequency-domain equalization (FDE) based on minimum mean square error (MMSE) criterion. MMSE-FDE can obtain the frequency diversity gain and hence, improve the SC transmission performance [3, 4]. In a cellular network, however, the same frequency is reused in different cells and the presence of co-channel interference (CCI) degrades the transmission performance. Adaptive antenna array (AAA) is a well-known technique to suppress the CCI [5]–[7]. Recently, we proposed a frequency-domain AAA (based on the average CCI power minimization criterion) jointly used with MMSE-FDE, for SC transmission [8]. In the proposed frequency-domain AAA, the received signal on each antenna is transformed into the frequency-domain signal by using fast Fourier transform (FFT) and the same array weight is used for all frequencies to adaptively form an antenna beam to suppress the CCI. The array weight is updated using the pilot which is transmitted regularly. Despite of using the simple normalized least mean square (NLMS) algorithm [9], very fast weight convergence is achieved.

In this paper, we theoretically derive the optimum array weight based on the average CCI power minimization criterion using Lagrange multiplier method [9]. Then, we evaluate, by computer simulation, the outage probability of the BER in a frequency-selective CCI environment.

II. SINGLE-CARRIER FREQUENCY-DOMAIN ADAPTIVE ANTENNA ARRAY

A. Transmitter structure

The transmitter structure is illustrated in Fig. 1. Binary data sequence is transformed into a data-modulated symbol sequence and divided into a sequence of blocks of N_c data symbols. The last N_g symbols in each block of N_c symbols are copied and inserted as a cyclic prefix into the guard interval (GI) which is placed at the beginning of each block, as shown in Fig. 2 [3, 4]. For array weight updating, a group of N_p pilot blocks is transmitted every N_d data blocks for array weight updating.

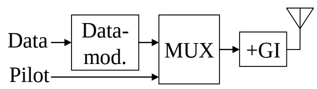

Figure 1. Transmitter structure.

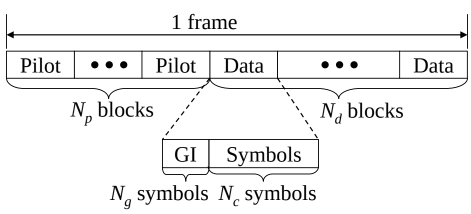

Figure 2. Frame structure.

B. Receiver structure

The transmitted signal is received through a frequency-selective block Rayleigh fading channel having L distinct paths with different time delays. The receiver structure using the frequency-domain AAA is illustrated in Fig. 3. M-antenna linear array is considered (see Fig. 4). The received signal vector $\mathbf{r}(t)=[r_0(t),\ \ r_1(t),\ \ \cdots\ \ r_{M-1}(t)]^T$ at time t can be expressed as

$$\begin{aligned}\mathbf{r}(t)&=\sqrt{2P_0}\sum_{l=0}^{L-1}\mathbf{h}_{0,l}s_0(t-\tau_{0,l})\\&+\sum_{u=1}^{U-1}\sqrt{2P_u}\sum_{l=0}^{L-1}\mathbf{h}_{u,l}i_u(t-\tau_{u,l})+\boldsymbol{\eta}(t)\end{aligned}, \quad (1)$$

where U is the number of users (including the desired user), P_u is the average received power of the uth user (u=0~U−1), $\mathbf{h}_{u,l}=[h_{u,l,0},h_{u,l,1},\cdots h_{u,l,M-1}]^T$ is the $(M\times1)$ lth path complex-valued path gain vector and $\tau_{u,l}$ is the lth path time delay. $s_0(t)$ and $\{i_u(t);u=1\sim U-1\}$ are the desired user's signal and the uth CCI, respectively. $\boldsymbol{\eta}(t)$ is a $(M\times1)$ noise vector characterized by zero-mean complex Gaussian variables with the variance $2N_0/T_s$, where N_0 is the single-sided power spectrum density of the additive white Gaussian noise (AWGN) and T_s is the symbol length. We assume that the fading statistics on each antenna is identical and

$$E[|h_{u,l,m}|^2]=\Omega_{u,l}\ \ \text{for}\ m=0\sim M-1 \quad (2)$$

with $\sum_{l=0}^{L-1}\Omega_{u,l}=1$.

After removing the GI, N_c-point FFT is applied. The frequency-domain received signal vector $\mathbf{R}(k)=[R_0(k),\ \ R_1(k),\ \ \cdots\ \ R_{M-1}(k)]^T$, k=0~N_c–1, at frequency k is expressed as

$$\begin{aligned}\mathbf{R}(k)&=\sum_{t=0}^{N_c-1}r(t)\exp\left(-j2\pi k\frac{t}{N_c}\right)\\&=\sqrt{2P_0}\mathbf{H}_0(k)S_0(k)+\sum_{u=1}^{U-1}\sqrt{2P_u}\mathbf{H}_u(k)I_u(k)+\boldsymbol{\Pi}(k)\end{aligned}. \quad (3)$$

In Eq. (2), $\mathbf{H}_u(k)$, $S_0(k)$, $I_u(k)$, and $\boldsymbol{\Pi}(k)$ are an $(M\times1)$ channel gain vector, the desired signal, the uth CCI, and an $(M\times1)$ noise vector. They are given as

$$\begin{cases}\mathbf{H}_u(k)=\sum_{l=0}^{L-1}\mathbf{h}_{u,l}\exp\left(-j2\pi k\frac{\tau_{u,l}}{N_c}\right)\\ S_0(k)=\sum_{t=0}^{N_c-1}s_0(t)\exp\left(-j2\pi k\frac{t}{N_c}\right)\\ I_u(k)=\sum_{t=0}^{N_c-1}i_u(t)\exp\left(-j2\pi k\frac{t}{N_c}\right)\\ \boldsymbol{\Pi}(k)=\sum_{t=0}^{N_c-1}\boldsymbol{\eta}(t)\exp\left(-j2\pi k\frac{t}{N_c}\right)\end{cases}. \quad (4)$$

The same array weight vector $\mathbf{w}$ is used for all frequencies (because of this, very fast weight convergence is achieved despite of using the simple NLMS algorithm). The array combiner output $Y(k)$ is expressed as

$$\begin{aligned}Y(k)&=\mathbf{w}^T\mathbf{R}(k)\\&=\sqrt{2P_0}\mathbf{w}^T\mathbf{H}_0(k)S_0(k)\\&+\sum_{u=1}^{U-1}\sqrt{2P_u}\mathbf{w}^T\mathbf{H}_u(k)I_u(k)+\mathbf{w}^T\boldsymbol{\Pi}(k)\end{aligned} \quad (5)$$

with $\|\mathbf{w}\|^2=1$, where the first term is the desired signal component, the second is the CCI, and the third is the noise. After array combining, MMSE-FDE is carried out as

$$\hat{Y}(k)=Y(k)w_{FDE}(k), \quad (6)$$

where $w_{FDE}(k)$ is the FDE weight, which can be derived as [10]

$$w_{FDE}(k)=\frac{(\mathbf{w}^T\mathbf{H}_0(k))^*}{|\mathbf{w}^T\mathbf{A}_0|^2+(P_0/\sigma^2)^{-1}}. \quad (7)$$

In Eq. (7), $\mathbf{A}_0=[1\ \ A_{0,l}\ \ \cdots\ \ A_{0,l}^M]^T$ is the steering vector associated with the desired user (u=0) with

$$A_{0,l}=\exp\left(j\pi\cos\theta_{0,l}\right), \quad (8)$$

where $\theta_{0,l}$ is the arrival angle of the lth path and we have assumed that the antenna separation is half the carrier wavelength. In Eq. (7), σ^2 is the sum of the average residual CCI power (which is not frequency-dependent) and the noise power and is given as

$$\sigma^2=\sum_{u=1}^{U-1}P_u|\mathbf{w}^T\mathbf{A}_u|^2+\frac{N_0}{T_s}. \quad (9)$$

After performing N_c-point inverse FFT (IFFT) on $\{\hat{Y}(k);k=0\sim N_c-1\}$, data-demodulation is carried out to recover the transmitted data symbol.

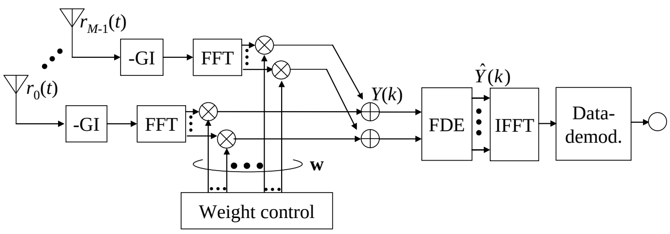

Figure 3. Receiver structure

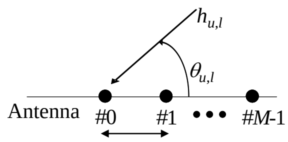

Figure 4. Linear antenna array.

C. NLMS algorithm

The NLMS algorithm [9] is used to update the array weight vector **w** using N_p pilot blocks. The nth weight updating can be done *in the frequency-domain* as

$$\begin{cases} \mathbf{w}'_n = \mathbf{w}_{n-1} + 2\mu e(k)\dfrac{\mathbf{R}^*(k)}{\|\mathbf{R}(k)\|^2} \\ \mathbf{w}_n = \dfrac{\mathbf{w}'_n}{\|\mathbf{w}'_n\|^2} \end{cases}, \tag{10}$$

where $k = n \bmod N_c$, $\|.\|$ is the vector norm operation, and μ is the step size parameter. In Eq. (10), $e(k)$ is the error signal. The array desired signal component $\sqrt{2P_0}\mathbf{w}_{n-1}^T\mathbf{H}_0 S_0(k)$ in the array combiner output $Y(k) = \mathbf{w}_{n-1}^T\mathbf{R}(k)$ is used as the reference [11, 12]. $e(k)$ can be expressed as

$$e(k) = \sqrt{2P_0}\mathbf{w}_{n-1}^T\mathbf{H}_0 S_0(k) - \mathbf{w}_{n-1}^T\mathbf{R}(k), \tag{11}$$

Since the array weight vector **w** doesn't need to track the fading and furthermore, weight updating can be done as many as N_c times during one pilot block (see Eq. (10)), very fast weight convergence can be achieved despite of using the simple NLMS algorithm.

The weight convergence rate is shown for N_c=1024, μ=1/32, and M=8 in Fig. 5. The mean square error between the optimum array weight vector $\mathbf{w}_{opt}$ (which will be derived in Sect. III) and the array weight vector $\mathbf{w}_n$ obtained by NLMS algorithm is plotted. In Fig. 5, we assumed one desired user and 6 co-channel users; the arrival angle of the desired user's signal is 0 degree, whereas those of CCI are 30, 90, 150, 210, 270, and 330 degrees. The average E_b/N_0 of the desired user's signal is 20 dB and the average signal-to-CCI power ratio (SIR) is set to 0 dB. Since N_c=1024 times of updating can be done during 1 pilot block, very fast weight convergence is observed; the array weight converges close to $\mathbf{w}_{opt}$ within 2 blocks as was expected. A possible reason why $\mathbf{w}_n$ does not approach an exact value of $\mathbf{w}_{opt}$ is that $\mathbf{w}_n$ is updated by noise and randomly phase-rotated when the CCI is sufficiently suppressed.

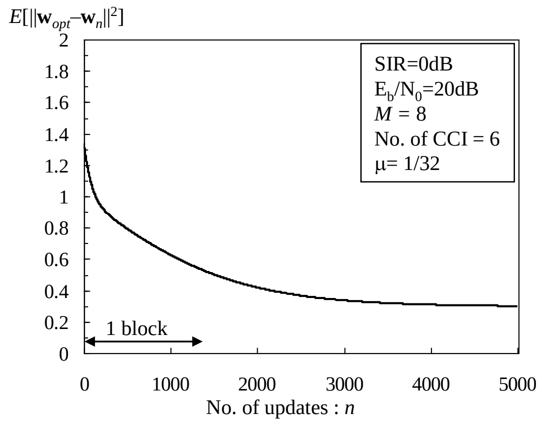

Figure 5. Array weight convergence rate.

III. ARRAY WEIGHT ANALYSIS

We use the cost function $J(\mathbf{w})$ which is defined in [13] as

$$J(\mathbf{w}) = E[|e(k)|^2] + \kappa(1 - \|\mathbf{w}\|^2), \tag{12}$$

where κ is the Lagrange multiplier [9]. Substituting Eq. (2) into Eq. (11), $e(k)$ can be written as

$$e(k) = -\sum_{u=1}^{U-1}\sqrt{2P_u}\mathbf{w}^T\mathbf{H}_u(k)I_u(k) - \mathbf{w}^T\mathbf{\Pi}(k). \tag{13}$$

We can show

$$E[|e(k)|^2] = \mathbf{\Phi}_{ii} + \mathbf{\Phi}_{nn}, \tag{14}$$

which is the same for all k. $\mathbf{\Phi}_{ii}$ and $\mathbf{\Phi}_{nn}$ are $M \times M$ auto-correlation matrices of the CCI and the noise, respectively, and are given as

$$\begin{cases} \mathbf{\Phi}_{ii} = \sum_{u=1}^{U-1} 2P_u E[\mathbf{H}_u^*(k)\mathbf{H}_u^T(k)] \\ \quad = 2P_u\sum_{u=1}^{U-1}\begin{bmatrix} 1 & \cdots & \sum_{l=0}^{L-1}\Omega_{u,l}A_{u,l}^{M-1} \\ \vdots & \ddots & \vdots \\ \sum_{l=0}^{L-1}\Omega_{u,l}A_{u,l}^{-(M-1)} & \cdots & 1 \end{bmatrix} \\ \mathbf{\Phi}_{nn} = E[\mathbf{\Pi}^*(k)\mathbf{\Pi}^T(k)] = \dfrac{2N_0}{T_s}\mathbf{I} \end{cases}, \tag{15}$$

where $\Omega_{u,l} = E[|h_{u,l}|^2]$ is defined by Eq. (2). The optimum weight can be derived by setting $\partial J/\partial\mathbf{w}^* = \mathbf{0}$. We can show that $\mathbf{w}_{opt}$ satisfies

$$(\mathbf{\Phi}_{ii} + \mathbf{\Phi}_{nn})\mathbf{w} = \kappa\mathbf{w}, \tag{16}$$

where the Lagrange multiplier κ corresponds to an eigen value of $\mathbf{\Phi}_{ii} + \mathbf{\Phi}_{nn}$. From Eq. (16), we obtain

$$\mathbf{w}^H(\mathbf{\Phi}_{ii} + \mathbf{\Phi}_{nn})\mathbf{w} = \kappa. \tag{17}$$

Since $\mathbf{w}^H(\mathbf{\Phi}_{ii} + \mathbf{\Phi}_{nn})\mathbf{w}$ is the (CCI+ noise) power after the array combining, the optimum array weight vector $\mathbf{w}_{opt}$ is an eigen vector corresponding to the minimum eigen value κ_{min} of $\mathbf{\Phi}_{ii} + \mathbf{\Phi}_{nn}$. Since the noise power is constant due to the constraint $\|\mathbf{w}\|^2 = 1$, the optimum array weight vector $\mathbf{w}_{opt}$ minimizes the average CCI power after the array combining.

IV. COMPUTER SIMULATIONS

A. Simulation set up

We consider a hexagonal cellular layout as shown in Fig. 6 and one user in each cell is communicating with its base station (BS) located in the center of a cell. The same frequency is reused at different cells; the cluster size F of 4 ~ 13 is considered in the simulation. The u=0th BS (center cell) is a cell of interest. We consider the CCI from the nearest U=6 co-channel cells, u=1~6, surrounding the u=0th BS.

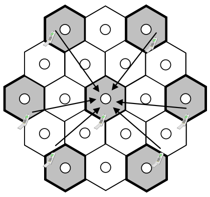

Figure 6. Cellular structure with F = 4.

Table I Simulation condition

Transmitter	Data modulation	QPSK
	No. of symbols	N_c = 1024
	No. of pilot blocks	N_p = 5
	Slow TPC	Target $SNR \rightarrow \infty$
Channel	Channel model	Frequency-selective block Rayleigh fading
	No. of paths	L = 16
	Time delay	τ_l=l, l = 0~L–1
	Path loss exponent	α = 3.5
	Standard deviation of shadowing losses	σ = 6 (dB)
Receiver	Antenna disposition	linear
	Antenna separation	d = 0.5λ
	Step size parameter	μ = 1/32

Table I summarizes the simulation condition. SC block transmission using QPSK data modulation and N_c=1024 symbols is considered. N_p=5-block pilot is transmitted for obtaining the array weight vector **w**. A sample-spaced L=16-path block Rayleigh fading with uniform power delay profile ($\Omega_{u,l}=1/L$) and the lth path time delay of $\tau_{u,l}$=l samples is assumed. Furthermore, the arrival angle spread of L paths is assumed to be negligibly small. Slow transmit power control (TPC) is assumed. Step size parameter of the NLMS algorithm is set to μ=1/32 for updating the array weight vector **w**.

Computer simulation is performed as follows. The locations of U co-channel users, one in each co-channel cell, and one desired user are randomly generated, and the shadowing losses and path gains to the u=0th BS are generated. Assuming slow TPC, the uth user's power P_u from the u^{th} MS received by the u=0th BS is computed using

$$P_u=\left(\frac{P}{d_{u\_u}^{-\alpha}\times 10^{-\frac{\eta_{u\_u}}{10}}}\right)\times d_{u\_0}^{-\alpha}\times 10^{-\frac{\eta_{u\_0}}{10}}\ , \quad (18)$$

where P is the TPC target power, d_{u_u} and η_{u_u} are respectively the distance and the log-normally distributed shadowing loss between the uth user and its BS, α is path loss exponent, and d_{u_0} and η_{u_0} are respectively the distance and the shadowing loss between the uth user and the u=0th BS. (In this paper, the interference-limited condition is assumed, i.e., Target $SNR \rightarrow \infty$.) Then, the path gain vector $\mathbf{h}_{u,l}$ for the lth path is generated. Substituting P_u, $\mathbf{h}_{u,l}$ and $\tau_{u,l}$ together with the Gaussian noise vector $\boldsymbol{\eta}(t)$ into Eq. (3), the frequency-domain received signal vector $\mathbf{R}(k)$ is generated. Then, the array weight updating following Eq. (10) is performed using N_p=5-block pilot. Using the generated array weight **w**, the average BER is computed. The above procedure is repeated a sufficient number of times by changing the MSs' locations, shadowing losses and path gains to obtain the distribution of the average BER.

B. *Outage Probability*

Figure 7 plots the outage probability which is defined as the probability of the measured average BER being more than abscissa. As the number M of antennas increases, the outage probability decreases. The frequency-domain AAA is seen to very effective to suppress the CCI. Since the dominant co-channel cells are the nearest 6 co-channel cells (therefore, only 6 co-channel cells are considered in this paper), the use of M=7 is sufficient to suppress the CCI. It can be seen from the figure that additional reduction of the outage probability by increasing M from 6 to 8 is small. For the cluster size of 4, the outage probability at average BER=10^{-3} reduces from 0.733 to 0.073 by using M=8 antennas. Similar improvement can be seen for the cluster size of 7.

C. *Reducing the cluster size*

The frequency efficiency of the cellular system can be improved by reducing the cluster size F. F is determined so as to keep the outage probability for the required average BER at the prescribed value.

In this paper, we assume the outage probability of 0.1 at the required average BER=10^{-3} (i.e., we allow the measured average BER to drop below 10^{-3} with a probability of 0.1). As the number M of antennas increases, the CCI can be better suppressed and therefore the co-channel cells can be located closer to each other, thereby decreasing the value of F. Figure 8 plots F as a function of M. When the single antenna is used (M=1), the allowable cluster size is F=13. Smaller F can be used by increasing M; the allowable cluster size is F=4 when M=8. The frequency efficiency can be increased by three times by using M=8 antennas.

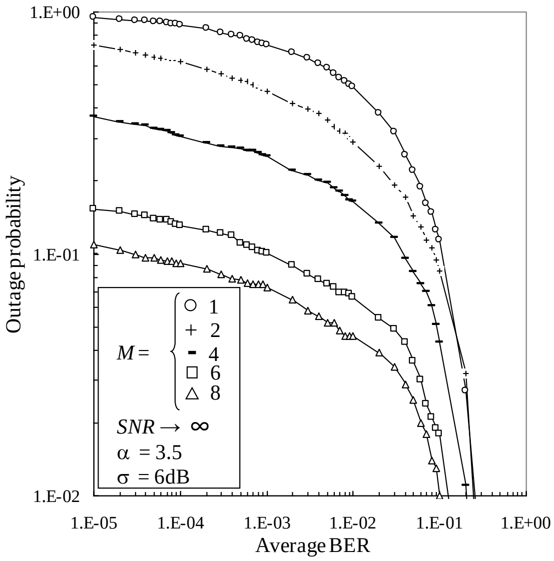

(a) $F = 4$

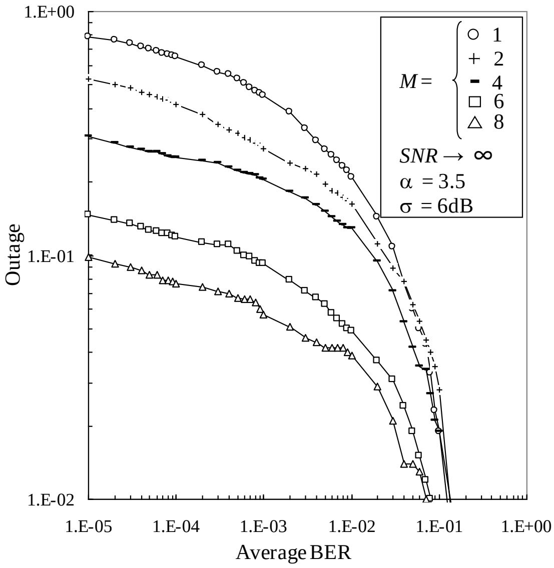

(b) $F = 7$

Figure 7. Outage probability.

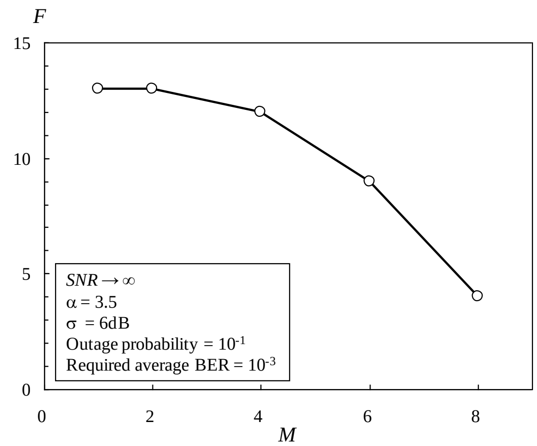

Figure 8. F as a function of M.

V. CONCLUSIONS

In this paper, we presented the single-carrier frequency-domain AAA jointly used with FDE for a cellular system to show how effectively suppress the CCI from co-channel cells and increase the spectrum efficiency. After transforming the received signal into a frequency-domain signal, array combining is done in the frequency-domain followed by FDE. The same array weight is used for all frequencies and the desired signal component after array combining is used as the reference signal for array weight updating. We theoretically derived the optimum array weight based on the average CCI power minimization criterion. We have shown that the optimum array weight is the eigen vector corresponding to the minimum eigen value of the auto-correlation matrix of CCI plus noise. We have shown by the computer simulation that a very fast weight convergence can be achieved despite of using the simple NLMS algorithm. Furthermore, we have shown that the frequency efficiency can be increased by three times by using M=8 antennas for the outage probability of 0.1 at the required average BER=10^{-3}.

REFERENCES

[1] W.C Jakes Jr, Ed, *Microwave mobile communications*, Wiley, New York, 1974.

[2] S. Hara and R. Prasad, "Overview of multicarrier CDMA," IEEE Commun. Mag., vol.35, no.12, pp.126-144, Dec. 1997.

[3] D. Falconer, S. L. Ariyavisitakul, A. Benyamin-Seeyaran and B. Eidson, "Frequency domain equalization for single-carrier broadband wireless systems," IEEE Commun. Mag., Vol. 40, pp.58-66, Apr. 2002.

[4] K. Takeda, T. Itagaki, and F. Adachi, "Joint use of frequency-domain equalization and transmit/receive antenna diversity for single-carrier transmissions," IEICE Trans. Commun., vol. E87-B, No. 7, pp.1946-1953, Jul. 2004.

[5] J.C. Liberti and T.S. Rappaport, *Smart Antennas for Wireless Communications*: *IS-95 & 3rd Generation CDMA Applications*, Prentice Hall, 1999.

[6] L.C. Godara, "Application of antenna arrays to mobile communications, Part I: Performance improvement, feasibility, and system considerations." Proc. IEEE, vol.85, no.7, pp.1029-1060, July 1997.

[7] L.C. Godara, "Application of antenna arrays to mobile communications, Part II: Beam-forming and direction of arrival consideration," Proc. IEEE, vol.85, no.8, pp.1195-1245, Aug. 1997.

[8] K. Takeda, R. Kawauchi, and F. Adachi, "Frequency-domain adaptive antenna array for single-carrier uplink transmission using frequency-domain equalization," Proc. WPMC2006, San Diego, U.S.A., 17-20 Sept. 2006.

[9] S. Haykin, *Adaptive Filter Theory*, 4th ed., Prentice Hall, 2001.

[10] K. Takeda and F. Adachi, "MMSE frequency-domain equalization combined with space-time transmit diversity and antenna receive diversity for DS-CDMA," Proc. 59th IEEE Vehicular Technology Conference (VTC), Milan, Italy, May 2004.

[11] S. Tanaka, M. Sawahashi, and F. Adachi, "Pilot symbol-assisted decision-direct coherent adaptive array diversity for DS-CDMA mobile radio reverse link," IEICE Trans. Commun., Vol.E80-A, No.12, pp.2445-2454, Dec. 1997.

[12] Y. Suzuki, E. Kudoh and F. Adachi, "Impact of arrival angle spread of an adaptive antenna array and antenna diversity in DS-CDMA mobile radio," IEICE Trans. Commun., Vol.E-87-B, No.4, pp.1037-1040. Apr. 2004.

[13] O. Nakamura, S. Takaoka, E. Kudoh, and F. Adachi, "Frequency-domain adaptive antenna array for multi-code MC-CDMA," IEICE Trans. Commun., Vol.E-90B, No.4, pp.918-925. Apr. 2007.